

Purdue University
Purdue e-Pubs

International Refrigeration and Air Conditioning
Conference

School of Mechanical Engineering

2018

Optimization Of Foam Characteristics For Falling Film Evaporators

Jayakumar Arjun

Indian Institute Of Technology Madras, India, arjunjk91@gmail.com

Mani Annamalai

mania@iitm.ac.in

Follow this and additional works at: <https://docs.lib.purdue.edu/iracc>

Arjun, Jayakumar and Annamalai, Mani, "Optimization Of Foam Characteristics For Falling Film Evaporators" (2018). *International Refrigeration and Air Conditioning Conference*. Paper 1922.

<https://docs.lib.purdue.edu/iracc/1922>

This document has been made available through Purdue e-Pubs, a service of the Purdue University Libraries. Please contact epubs@purdue.edu for additional information.

Complete proceedings may be acquired in print and on CD-ROM directly from the Ray W. Herrick Laboratories at <https://engineering.purdue.edu/Herrick/Events/orderlit.html>

Optimization of Foam Characteristics for Falling Film Evaporators

Arjun Jayakumar, Mani A*

Refrigeration and Air conditioning Laboratory, Department of Mechanical Engineering,
Indian Institute of Technology, Madras, India.

*Corresponding author. Tel.:+91 44 22574666; fax: +91 44 22570509
Email address: mania@iitm.ac.in

ABSTRACT

Numerical analysis of horizontal tube falling film evaporation over metal foam wrapped evaporator tubes was carried out and found to enhance the heat transfer. Metal foam characteristics like porosity and permeability was optimized to give maximum heat transfer rate. Computational analysis were carried out using commercial software. Optimization of foam characteristic was carried out at falling film Reynolds number of 650.

1. INTRODUCTION

There is an acute scarcity in availability of water across the world. One-fifth of the world's population, live in areas of physical water scarcity. Due to the natural constraints and conditions in the Middle East and Africa, fresh water is relatively scarce and similarly in the western developed regions, the original fresh water resources can hardly support the excessive pressure of the population (Jeuland, 2015). To meet this ever rising demand for fresh water, establishment of desalination plants is considered as one of the most feasible solution. Multi-Effect Desalination systems are thermal based system with Horizontal Falling Film Evaporators (HTFFEs). Falling films have the inherent advantage high heat transfer coefficient at small temperature differences, very low pressure drop of the liquid flowing over the tubes, and small quantity of working fluid required.

HTFFEs are featured by evaporation from the liquid film over the surface of the tube and simultaneous condensation inside the tube. Condensation heat transfer coefficient is higher than evaporative heat transfer and can be improved by using heat transfer enhancement technique (Abraham and Mani, 2015). Researchers have investigated on the techniques of improvement of evaporation side heat transfer. Porous layer coating of thickness 800 μ m were applied on the heat exchanger tubes by Bogan and Park (2014). Complete wetting of evaporator tube was obtained by the capillary action of the pore and thus enhances the heat transfer. Rough surface configuration, ranging from random sand-grain-type roughness to discrete protuberances, for heat transfer enhancement were investigated (Tewari *et al.*, 1986, Zheng and Worek, 1996, Li *et al.*, 2011). Rough surfaces promote turbulence and more surface area for heat transfer. Evaporators with thermal spray coated Aluminium tubes were found to give 75-150% increase in heat transfer rate compared to plain tube (Abraham and Mani, 2014).

Metal foams, a class of materials, featured by high porosity are finding applications in the field of process industries and power cycles due to their higher surface area and tortuous flow path. Metal foams have a periodic structure formed by metal struts commonly in Aluminium, Nickel or Copper. Air flow experiments over tubes wrapped with metal foams are found to have better performance compared to helically finned tubes (T'Joel *et al.*, 2010). Application of metal foams in falling film evaporators were investigated by Arjun and Mani (2017). Enhancement of heat and mass transfer by 150% was predicted. The drawback of higher pressure drop while using metal foams in air heat exchangers is not present when used in falling film evaporators as the flow is dominated by gravity and thus heat transfer enhancement could be obtained without additional pumping power. Present study optimizes the foam characteristics, porosity and permeability, using numerical simulations. Enhancement in heat transfer was determined by comparing it with values from r evaporation over bare tube. Commercial CFD package was used for computation.

2. NUMERICAL SIMULATION

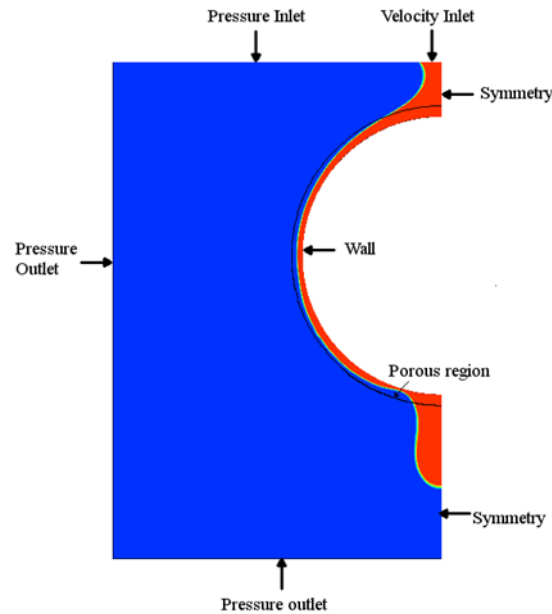


Figure 1: Falling film over horizontal tube domain and boundary condition

A single horizontal heated tube of diameter 25.4mm over which metal foam of 1mm thickness wrapped, is considered to optimize the foam parameters. Figure 1 shows the computational domain with contours of vapour (in blue) and liquid (in red) along with the boundary conditions applied. Only one half of the tube is modelled as there is flow symmetry. An isothermal boundary condition, 64.6°C, is used at wall boundary for solving energy equation and a non-slip boundary condition for momentum equation. Flow rate of liquid is determined by the velocity inlet boundary condition. All computations were carried out for falling film Reynolds number of 650 and at saturated condition corresponding to 62 °C. Sea water, salinity 35,000 ppm, properties are incorporated to the software using User Defined Functions (UDFs). An initial condition of 0.21 atm, saturation pressure corresponding to 62 °C, is applied to the domain. Residual value of 1×10^{-3} for continuity and momentum equation and 1×10^{-6} for energy equation is fixed as the convergence criteria. A time step of $1 \mu\text{s}$ is used in order to avoid divergence and instability.

Falling film evaporation over heated tube is simulated using Volume of Fluid (VOF) model. Wall superheat is small enough not to initiate nucleate boiling and the mass transfer is only by evaporation from the liquid surface. Evaporative mass transfer at the interface is captured using Rankine-Hugniot jump condition (Gibou *et al.*, 2007) and is added to the governing equations as source term via UDF. The assumptions involved in the governing equations of transport of fluid through metal foam are as follows: (i) flow is laminar (ii) effects of buoyancy and thermal dispersion are neglected (iii) uniform porosity within the porous medium (iv) change in momentum due to evaporation is neglected (v) mass transfer is only by evaporation from liquid film interface (v) local thermal equilibrium prevail between the lumped volume averaged temperature of the solid or fluid constituent. Governing equation of continuity, momentum and energy is given in Equation (1), (2) and (3) respectively. Source terms are added in continuity (S_M) and energy (S_E) equation to capture mass transfer due to evaporation.

$$\frac{\partial \rho}{\partial t} + \nabla \cdot (\rho \vec{u}) = S_M \quad (1)$$

$$\rho_f \left[\frac{1}{\phi} \right] \frac{\partial \vec{u}}{\partial t} + \frac{1}{\phi} \vec{u} \cdot \nabla \vec{u} = -\nabla P + \mu_e \nabla^2 \vec{u} + \rho g - \frac{u}{K} \vec{u} - \rho C |\vec{u}| \vec{u} \quad (2)$$

Gravitational term (third on RHS of Equation (2)) is applied only in the y-direction of flow. Fourth term on the RHS of Equation (2) accounts the contribution of permeability. These terms will be absent in case of bare tube simulation.

$$(\rho c)_s \frac{\partial T}{\partial t} + (\rho c_p)(\vec{u} \cdot \nabla T) = k_{eff} \nabla^2 T + \frac{\mu}{K} \phi + S_E \quad (3)$$

Energy source term due to evaporation of thin film is obtained by multiplying the mass flux with latent heat of vaporization. Local thermal equilibrium is considered since there is negligible temperature difference between fluid and solid part of porous media. Evaporative mass transfer at the interface in saturation condition is determined by the Rankine-Hugoniot jump condition proposed by Gibou *et al.*

$$m'' h_{fg} = -k \nabla T \cdot \vec{N} \quad (4)$$

volumetric mass source term as:

$$S_g = -S_f = \frac{k(\nabla \alpha \cdot \nabla T)}{h_{fg}} \quad (5)$$

and source term for energy equation as:

$$S_E = h_{fg} S_f \quad (6)$$

3. RESULTS AND DISCUSSION

3.1 Effect of porosity

Porosity is defined as the ratio of volume occupied by pore to the total volume of porous media. Effective thermal conductivity of metal foam is mostly given as a function of porosity. Calmidi and Mahajan (1999) have proposed an empirical relation for the effective thermal conductivity as a function of porosity and thermal conductivities of the constituent elements. This relation is given in Equation (7). Porosity is varied in the range 0.6 to 0.9 by keeping permeability value constant at $9e-8m^2$. Figure 2 shows the variation of average heat transfer coefficient with porosity. Maximum heat transfer coefficient is obtained at porosity value of 0.8. It is clear from Figure 2 that the heat transfer coefficient is not a linear function of porosity and there are competing effects which determine the final heat transfer rate. The competing effects are the effective thermal conductivity and the attainment of thermally developed region. As per the Equation (7) the effective thermal conductivity decreases with the increase in porosity and this decreases the heat transfer rate with metal foam having porosity of 0.9. At porosity value lower than 0.8, falling film over horizontal tube will attain thermally developed non-dimensional profile (Equation (8)) at early circumferential angle. Thermally developed region is characterized by lower heat transfer coefficient compared to preceding thermally developed region. As evident from the temperature profile shown in Figure 3 non-dimensional temperature profile remains close to unity at circumferential angles above 120° for foam porosity value of 0.8 and 90° for porosity 0.7. The lower temperature gradient available for heat transfer near the wall surface reduces the heat transfer rate at higher circumferential angles.

$$k_{eff} = \phi k_f + A(1 - \phi)^{0.763} k_s \quad (7)$$

where, $A=0.195$ for water

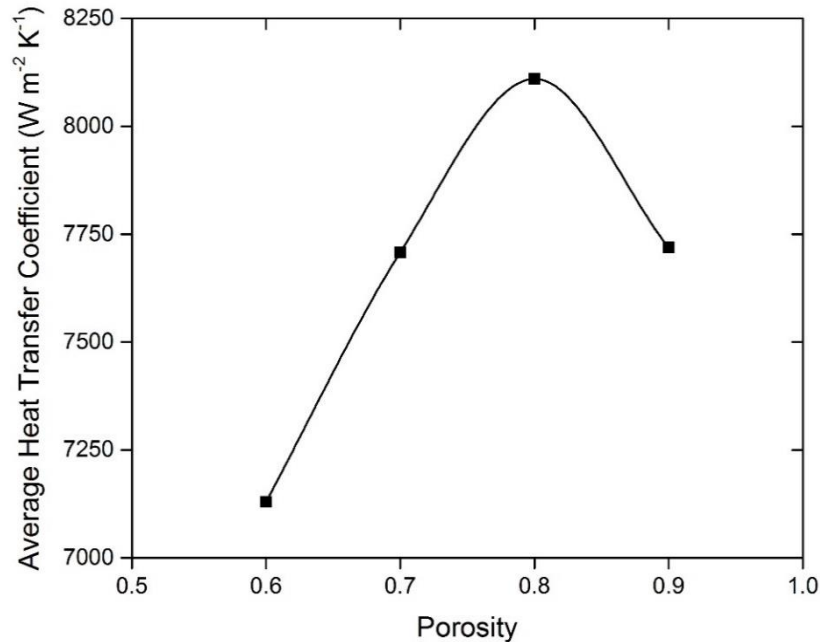


Figure 2: Variation of average heat transfer coefficient with foam porosity

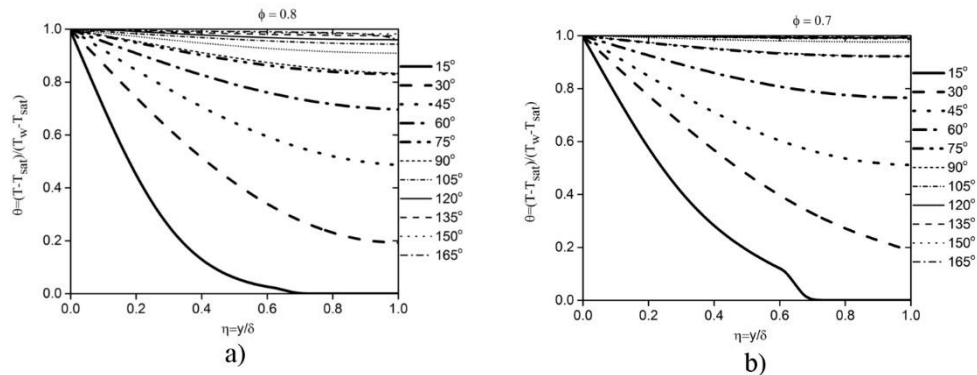


Figure 3: Non-dimensional temperature profile in horizontal falling film for foam porosity a) 0.8 and b) 0.6

Non-dimensional parameters θ and η are defined as:

$$\theta = \frac{T - T_{sat}}{T_w - T_{sat}}; \quad \eta = \frac{y}{\delta} \quad (8)$$

Foam wrapped tube having porosity of 0.8 increases the heat transfer rate by 2.5 times when compared with the bare tube. Figure 4 shows the variation of local heat transfer coefficient with circumferential position for bare and foam wrapped tube. A dip in the local heat transfer rate is predicted at the point where the inlet liquid hits the horizontal tube known as the top most stagnation point, which is assigned a circumferential angle of 0° . This is because a portion of the liquid will take a circumferential path through the porous media without hitting the stagnation point and resulting in lower heat transfer rate in that region. For the rest of the path falling liquid film will have higher heat transfer coefficient due to contribution from metal foam.

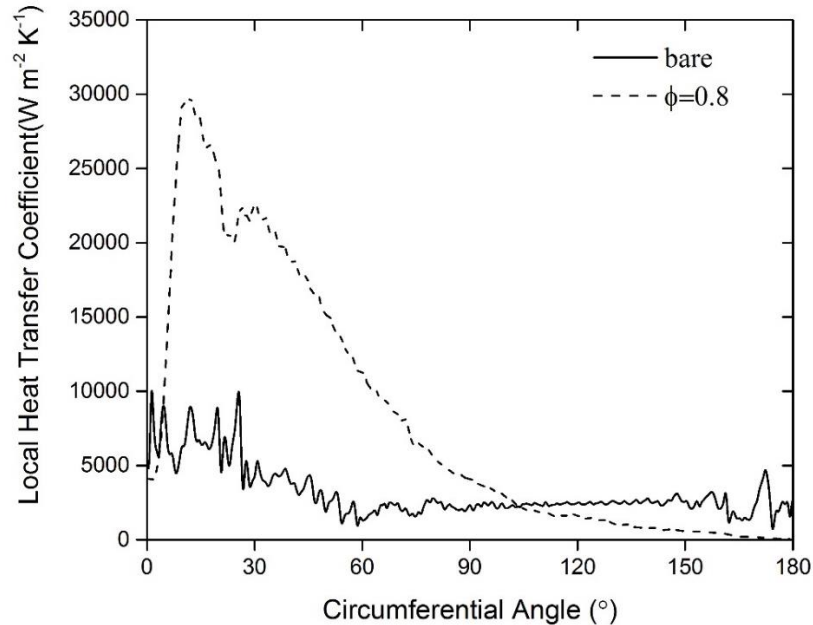


Figure 4: Circumferential variation of local heat transfer coefficient for bare and metal foam wrapped tube

3.2 Effect of permeability

Permeability characterizes the resistance to flow through the pores. Effect of permeability on heat transfer rate is investigated in the range $9e-7$ to $9e-9$ m^2 keeping porosity value constant at 0.9. Metal foams usually have a permeability in the range selected. Permeability of metal foams CFD simulations predict an increase in heat transfer rate with the permeability as shown in Figure 5. The increase in heat transfer coefficient is attributed to decrease in falling film thickness. Falling film thickness reduces with increase in permeability due to the easiness of flow associated with it. This reduction in film thickness will lead to reduction in conductive resistance across the film and thus increases the heat transfer coefficient. Figure 6 shows the circumferential variation of local film thickness for foams of different permeability. To calculate film thickness value radial lines from the wall surface is drawn at intervals of 15° circumferential angle to obtain the volume fraction values. Film thickness is fixed as the length between the wall surface and the position at which liquid volume fraction value drop to 0.5 from 1 along the radial line.

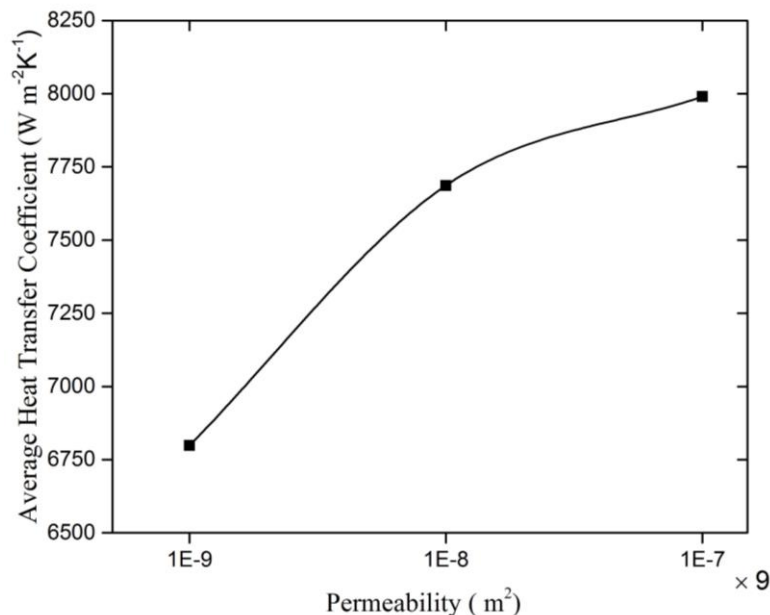


Figure 5: Variation of average heat transfer coefficient with permeability

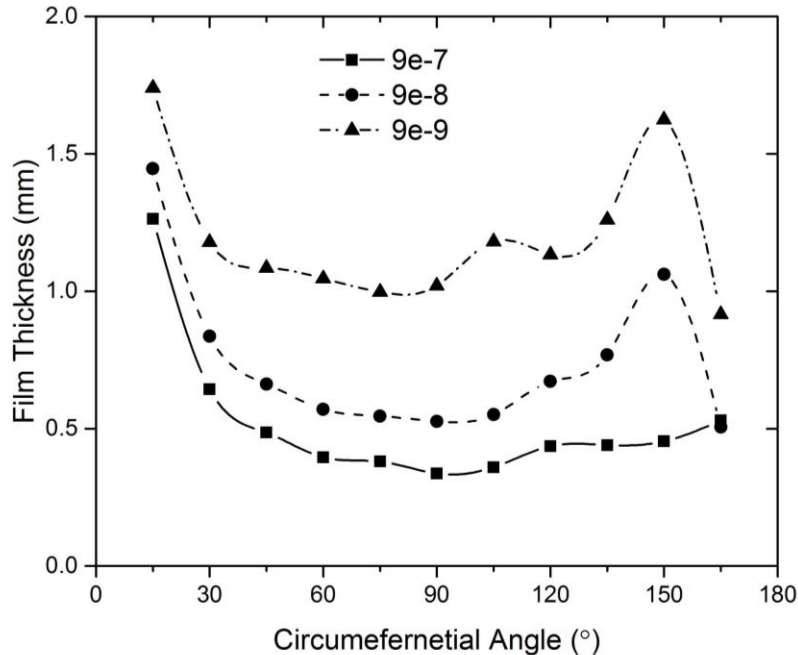


Figure 6: Circumferential variation of liquid film thickness for different foam permeability

3.3 Effect of flow rate and foam thickness

Computations were carried out at two flow rates and it was predicted that heat transfer rate increases with flow rate as shown in Figure 7. Metal foam thickness was varied between 1 mm to 1.75 mm where the heat transfer coefficient remains invariable to foam thickness. But a higher value of heat transfer coefficient is observed with foam of thickness of 1.25 mm. There are two competing effects, increase in the foam thickness allow more fluid to be in contact with the metal part which tends to increase heat transfer and simultaneously increase in foam thickness will also lead to increase in the conductive resistance due to increase in falling film thickness. For falling film Reynolds number for which computations were carried out an optimum is arrived at 1.25mm foam thickness.

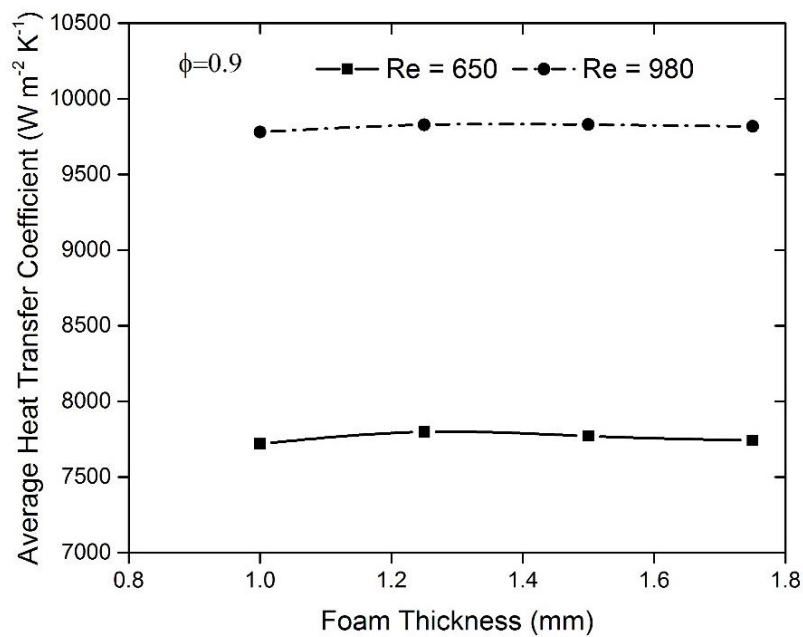


Figure 7: Variation of average heat transfer coefficient with falling film Reynolds number and foam thickness

4. CONCLUSIONS

It is evident from the study that metal foams are effective material for enhancing the heat transfer rate in horizontally falling film evaporators. Optimum value of foam porosity is predicted at 0.8 from CFD simulations. It increases the heat transfer rate by 2.5 times compared to bare tube. Effect of metal foam permeability is investigated at the order of magnitude 10^{-7} to 10^{-9} . It was predicted that heat transfer coefficient increases with permeability. Heat transfer rate increases with flow rate and have a slight advantage for a foam thickness of 1.25mm.

NOMENCLATURE

C	Form drag	(m)
g	acceleration due to gravity	(m/s ²)
h_{fg}	latent heat	(kJ/kg)
k	thermal conductivity	(W/m K)
K	permeability	(m ²)
\dot{m}	mass flux	(kg/m ² s)
P	pressure	(N/m ²)
Re	falling film Reynolds number, $2\Gamma/\mu$	(-)
S	source term	
t	time coordinate	(s)
T	temperature	(K)
u	velocity	(m/s)
ϕ	porosity	
Γ	liquid flow rate per unit length of cylinder flowing over horizontal tube	(kg/m s)
μ	dynamic viscosity	(kg/m s)

Subscript

eff	effective
f	fluid
s	solid
sat	saturation
w	wall

REFERENCES

- Abraham, R., & Mani, A. (2015). Heat transfer characteristics in horizontal tube bundles for falling film evaporation in multi-effect desalination system. *Desalination*, 375, 129-137.
- Abraham, R., & Mani, A. (2015). Experimental studies on thermal spray-coated horizontal tubes for falling film evaporation in multi-effect desalination system. *Desalination and Water Treatment*, 56(1), 71-82.
- Arjun, J. & Mani, A., (2017). Computational analysis of high porosity aluminium foam for heat and mass transfer enhancement in falling film evaporator. *6th Asian Symposium on Computational Heat Transfer and Fluid Flow (1-7)*. Indian Institute of Technology Madras, Chennai, India.
- Bogan, N., & Park, C. (2014). Influences of solution subcooling, wall superheat and porous-layer coating on heat transfer in a horizontal-tube, falling-film heat exchanger. *International Journal of Heat and Mass Transfer*, 68, 141-150
- Calmidi, V. V., & Mahajan, R. L. (1999). The effective thermal conductivity of high porosity fibrous metal foams. *Journal of Heat Transfer*, 121(2).
- Gibou, F., Chen, L., Nguyen, D., & Banerjee, S. (2007). A level set based sharp interface method for the multiphase incompressible Navier–Stokes equations with phase change. *Journal of Computational Physics*, 222(2), 536-555.
- Jeuland, M. (2015). Challenges to wastewater reuse in the Middle East and North Africa. *Middle East Development Journal*, 7(1), 1-25.
- Li, W., Wu, X. Y., Luo, Z., & Webb, R. L. (2011). Falling water film evaporation on newly-designed enhanced tube bundles. *International journal of heat and mass transfer*, 54(13-14), 2990-2997.

T'Joel, C., De Jaeger, P., Huisseune, H., Van Herzeele, S., Vorst, N., & De Paepe, M. (2010). Thermo-hydraulic study of a single row heat exchanger consisting of metal foam covered round tubes. *International Journal of Heat and Mass Transfer*, 53(15-16), 3262-3274.

Tewari, P. K., Verma, R. K., Ramani, M. P. S., & Mahajan, S. P. (1986). Effect of surface roughness & polymeric additive on nucleate pool boiling at subatmospheric pressures. *International communications in heat and mass transfer*, 13(5), 503-514.

Zheng, G. S., & Worek, W. M. (1996). Method of heat and mass transfer enhancement in film evaporation. *International Journal of Heat and mass transfer*, 39(1), 97-108.